

# THE EXPERIENCE OF THE CARTOGRAPHIC INSTITUTE OF CATALONIA (ICC) ON CONTINUOUS DINSAR MONITORING OF LARGE AREAS

Oscar Mora, Roman Arbiol, Vicenç Palà

*Institut Cartogràfic de Catalunya (ICC)*  
*Parc de Montjuïc, s/n, 08038 Barcelona, Spain*  
*Email: [oscar.mora@icc.cat](mailto:oscar.mora@icc.cat)*

## ABSTRACT

The Institut Cartogràfic de Catalunya (ICC) has developed an automatic advanced DInSAR processor (DISICC) for subsidence monitoring of large areas using data acquired by ERS-1/2, ENVISAT, and the future ALOS, TerraSAR-X and Radarsat 2 satellites. This processor performs the co-registration, interferogram generation, filtering, topographic cancellation, linear deformation model adjustment and non-linear displacement estimation, allowing the generation of classical and advanced DInSAR results combining information from different orbits and satellites. This new software is already operative and it is being used for a large project of continuous monitoring of subsidences in the whole territory of Catalonia (Spain).

## 1. INTRODUCTION

This paper presents a DInSAR project that uses 10 different ERS/ENVISAT frames, 5 descending and 5 ascending. These frames nearly cover the whole territory of Catalonia, see Fig. 1, which is about 31.930 Km<sup>2</sup>. The study is divided into two different processes. The first one is the generation of a stack of classical DInSAR data for each frame using moderate spatial baselines for minimizing phase decorrelation. The interferograms with short temporal gaps, i.e. less than six months, can be used for the identification of strong deformation areas, whose phase pattern is much higher than the atmospheric artifacts. The second step consists of the usage of this stack of differential interferograms with the advanced DInSAR processor implemented in ICC. This processor is capable of obtaining the subsidence velocity and the temporal deformation pattern minimizing the effects of atmospheric artifacts. Several DInSAR results obtained using this methodology are presented. They are compared with leveling measurements to demonstrate the excellent quality of the deformation maps obtained by advanced DInSAR processing.

## 2. GENERATION OF INSAR PAIRS

The criterion of pair generation has been the same for all 10 ascending and descending frames. For this project, a maximum spatial baseline of 150 meters and a maximum temporal gap of 8 years have been imposed.

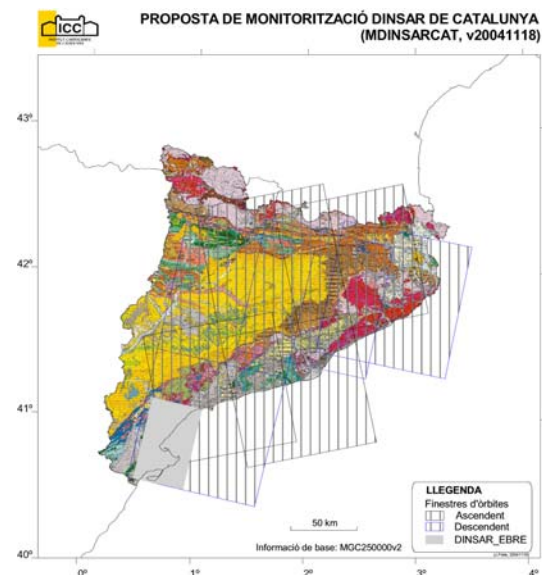


Figure 1. Ascending and descending frames covering the study area

Using this criterion the following interferograms have been generated (Tab. 1 and 2):

Ascending	SAR images	Interferograms
Track 015 Frame 0819	19	25
Track 244 Frame 0819	30	40
Track 244 Frame 0837	25	30
Track 473 Frame 0837	18	22
Track 201 Frame 0837	20	44

Table 1. Ascending interferograms

Descending	SAR images	Interferograms
Track 423 Frame 2781	30	49
Track 194 Frame 2781	19	35
Track 151 Frame 2763	19	35
Track 380 Frame 2763	20	43
Track 423 Frame 2763	37	89

Table 2. Descending interferograms

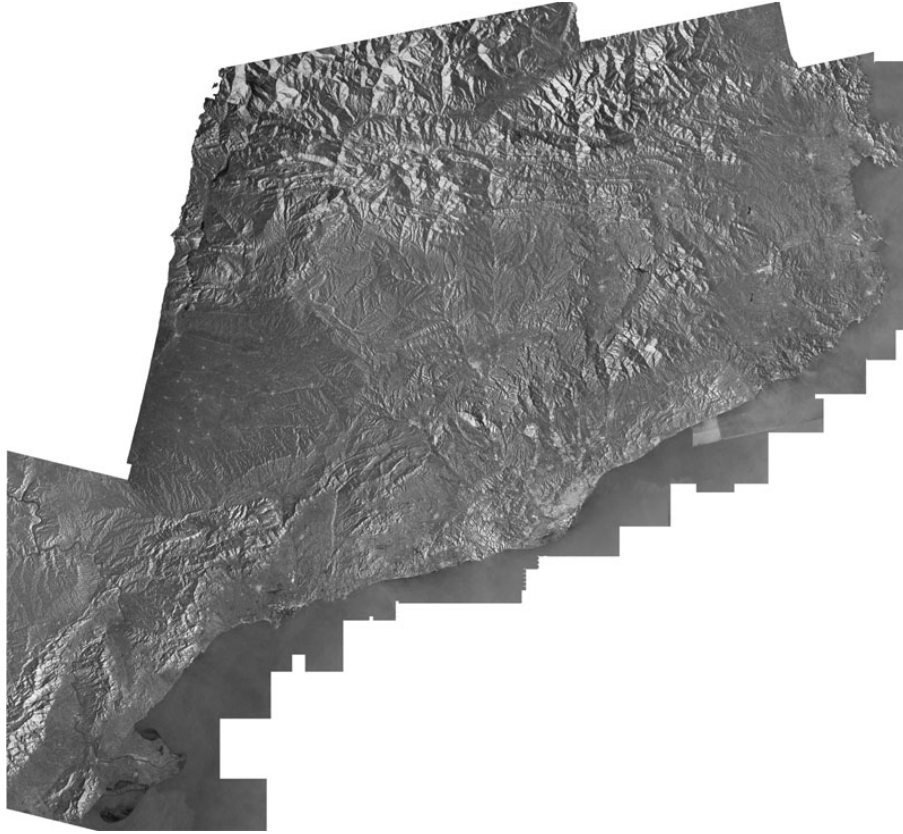


Figure 2. Radar orthoimage of Catalonia

After rectification, averaging and mosaicking of the amplitude images from the 10 frames, the radar orthoimage of Catalonia presented in Fig. 2 is obtained. Remark that the process for obtaining the mosaic is similar to the one used for optical images in the ICC [1].

### 3. DINSAR PROCESSING

The processing is divided into two parts, classical and advanced DInSAR [2]. At the same time, each part consists of the following steps:

#### 3.1. Classical DInSAR

- *Image registration*: All the SAR images corresponding to a same track and frame are registered respect to one of the images called super-master. This super-master is selected as the one with a centered orbit respect to the others.
- *Interferogram generation*: Once images are registered, the interferometric pairs are selected. Criteria are based on maximum spatial and temporal baselines, resulting in low temporal and spatial decorrelations, and consequently, phase quality is optimized.

- *Topographic removing*: Using a Digital Elevation Model (DEM) and the orbital information from SAR images the topographic interferometric phases are simulated and subtracted from the interferograms. The result is a stack of interferograms whose main phase component is due to terrain deformation. Nevertheless, this phase is contaminated with atmospheric artifacts and other noise sources, and therefore, only strong deformations can be successfully detected using classical DInSAR techniques.

#### 3.2. Advanced DInSAR

- *Selection of coherent pixels*: High quality pixels are selected based on coherence criterion taking into account the whole temporal stack of coherence maps. The subsidence estimation will only be performed over the selected pixels, not considering the rest.
- *Triangulation*: In order to reduce the impact of atmospheric artifacts a Delaunay triangulation is performed between the selected pixels. Therefore, the algorithm only works with interferometric phase increments between neighboring pixels.

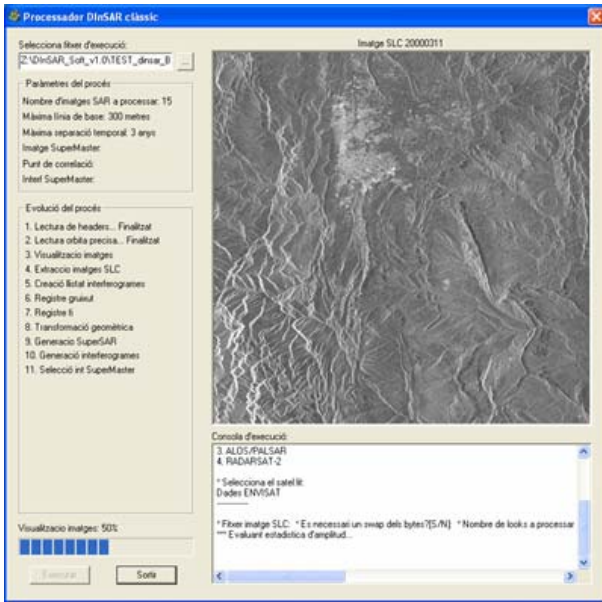


Figure 3. Classical DInSAR ICC's software

- **Linear deformation model:** A phase model is adjusted to phase increments taking into consideration only a linear deformation trend and the topographic residues of the DEM used for topographic cancellation [3]. At the same time, a measurement quality value is also obtained.
- **Integration:** Data integration is performed using the linear model adjustment and the triangulation structure, to obtain absolute values of deformation velocity and topographic error over the selected pixels. Those points with bad connections (low quality model) are rejected.
- **Residual estimation:** Once the linear model has been applied, the results are subtracted from the original interferometric phase increments, obtaining phase residues mainly composed by the non-linear deformation trend and a residual component of the atmospheric artifacts.
- **Non-linear deformation estimation:** Using the phase residues previously obtained, the system that relates interferometric phase pairs with absolute SAR phases is solved by means of the Single Value Decomposition (SVD) technique [4]. Then, the sum of the temporal residues and the linear model results in the determination of the temporal evolution of deformation.

This advanced DInSAR processing is iteratively applied using different coherence thresholds, and therefore, different levels of pixel selection. In the first iteration the pixel density is very high and mainly located in the urban areas, and in the last iteration density is decreased but more homogeneously distributed over the studied area. The different obtained solutions are merged to generate a complete deformation map of the area.

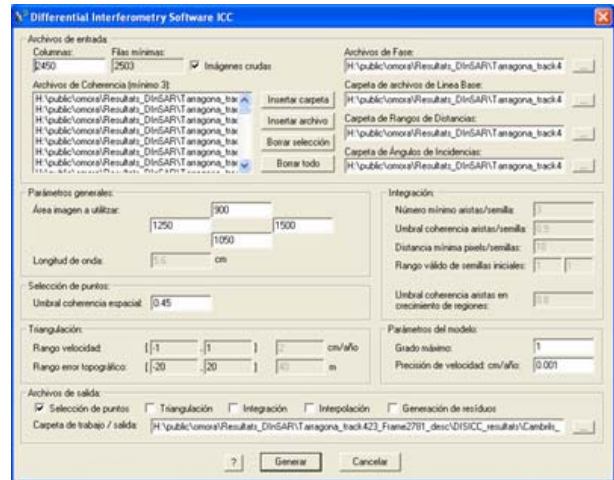


Figure 4. Advanced DInSAR ICC's software

Finally, a growing processing has been implemented to maximize the number of calculated points. In this case coherence criteria are not taken into account, and the advanced DInSAR algorithm is applied over all the rejected pixels located near the calculated ones. Iteratively, more and more pixels are estimated finishing when no more possible solutions are possible. Note that this procedure is like a region growing processing of the areas calculated in the first steps.

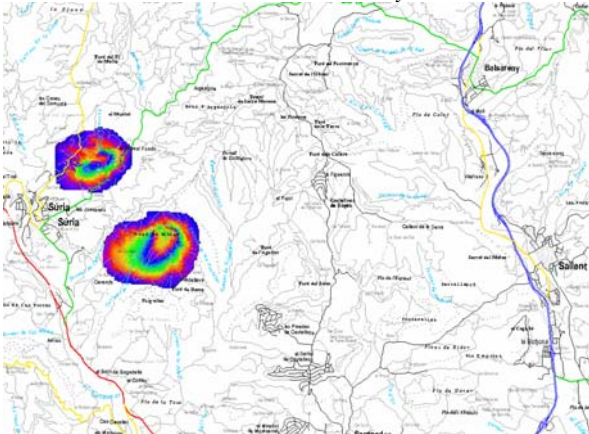
#### 4. CLASSICAL DINSAR RESULTS

Classical DInSAR is very useful for monitoring strong terrain displacements that generate much more phase fringes than atmospheric artifacts, for example. In those cases, short temporal baselines can be used due to the magnitude of the phenomenon, resulting in interferograms with very high coherence. Thus, vegetated areas that can not be studied by means of advanced techniques can be monitored for strong displacements using classical DInSAR.

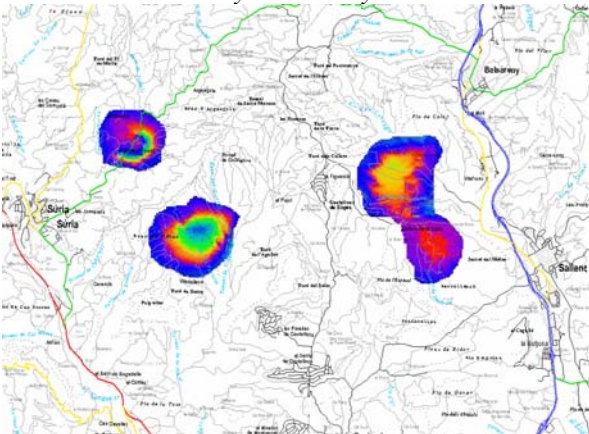
During the study of the Catalanian territory an area affected by this kind of subsidences has been detected. The results are shown in Fig. 5, where different phase fringes due to terrain subsidence are observed. Initially, only two areas were detected during 1993, but in 2005 a new subsidence zone appears as shown in Fig. 5. Moreover, a planimetric displacement on the deformation cones has been observed using the interferograms generated at different dates. Note that the temporal gap used for these interferograms is very short (1-3 months) in order to minimize temporal decorrelation. On the other hand, this configuration only allows detecting strong displacements, such as the ones depicted in Fig. 5 (larger than 30 cm/year), that in this case are caused by the subterranean mining works in the area.



December 1992 – January 1993



January – February 2005



February – May 2005

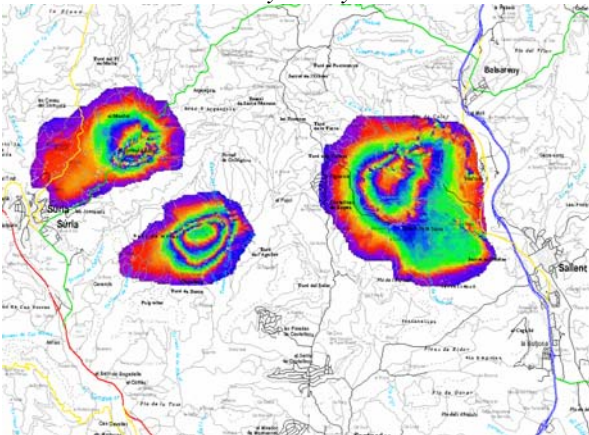


Figure 5. Deformation fringes (> 30 cm/year) generated by mine activities

## 5. ADVANCED DINSAR RESULTS

Previous results using classical DInSAR correspond to non-urban vegetated areas that are strongly subsiding. Nevertheless, slow movements can not be detected by means of short temporal baseline interferograms. For this reason advanced DInSAR techniques must be applied to the rest of the territory. In those cases, only high coherent areas in time can be monitored. For this

reason, the presented results correspond to urban zones and their surroundings.

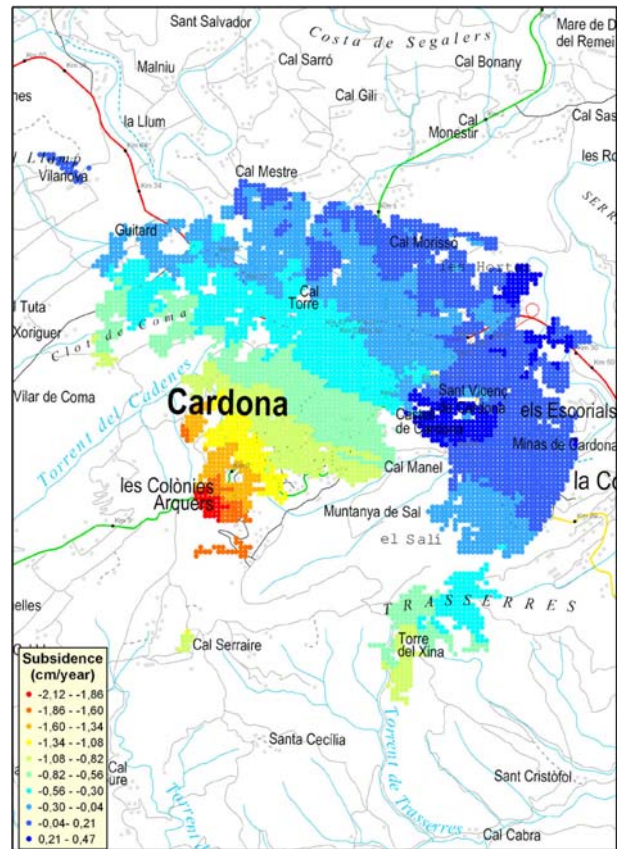


Figure 6. Deformation values for the town of Cardona

Fig. 6 shows the subsidence values for the coherent pixels in Cardona, a town located in the central part of Catalonia near the area presented in Fig. 5. Again, this subsidence is being caused by mining activity in the area. In this case the study has been performed over an urban area which is affected by a situation of risk for buildings.

Introducing all this information into a GIS environment, and taking into account the high density of coherent points, an interpolation of the results can be performed, obtaining the map presented in Fig. 7. All these data can be merged with other sources, such as orthophoto, to complete the information of the area under study (location, topography, etc.). Fig. 8 shows an example of the usage of the deformation maps obtained with advanced DInSAR techniques in the Google Earth environment. Using these formats information can be shared very easily with the final users.

Another example is the velocity deformation map shown in Fig. 9. It corresponds to a neighborhood in the south part of Sallent, near Cardona.



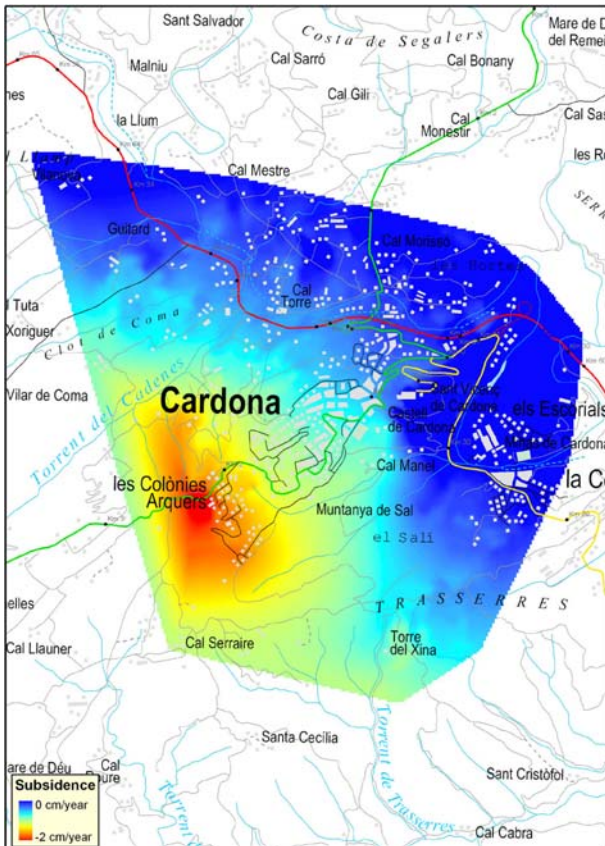


Figure 7. Interpolated deformation values for the town of Cardona

In the case of Sallent the deformation gradient is so high that some buildings have been demolished to avoid the risk of collapse. During the last years this area has been monitored using precise leveling measurements (see Fig. 10), allowing performing a velocity comparison between DInSAR and leveling. Tab. 3 shows the agreement between both methodologies.

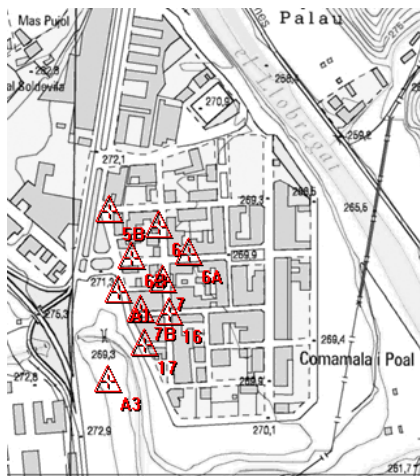


Figure 10. Points measured by means of precise leveling in Sallent

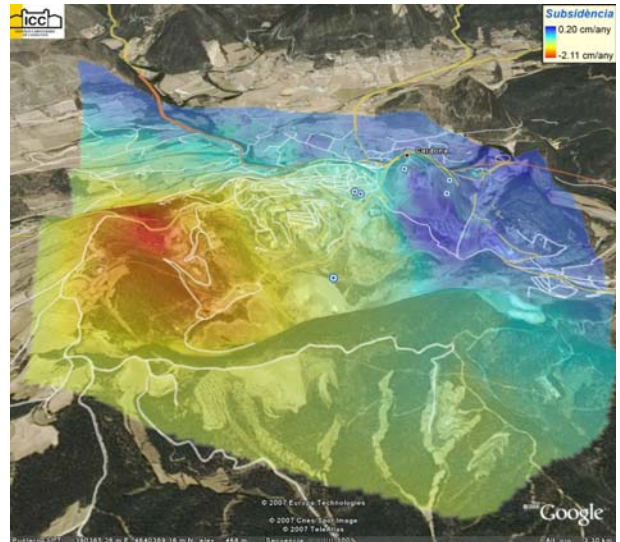


Figure 8. Subsidence map of Cardona in Google Earth

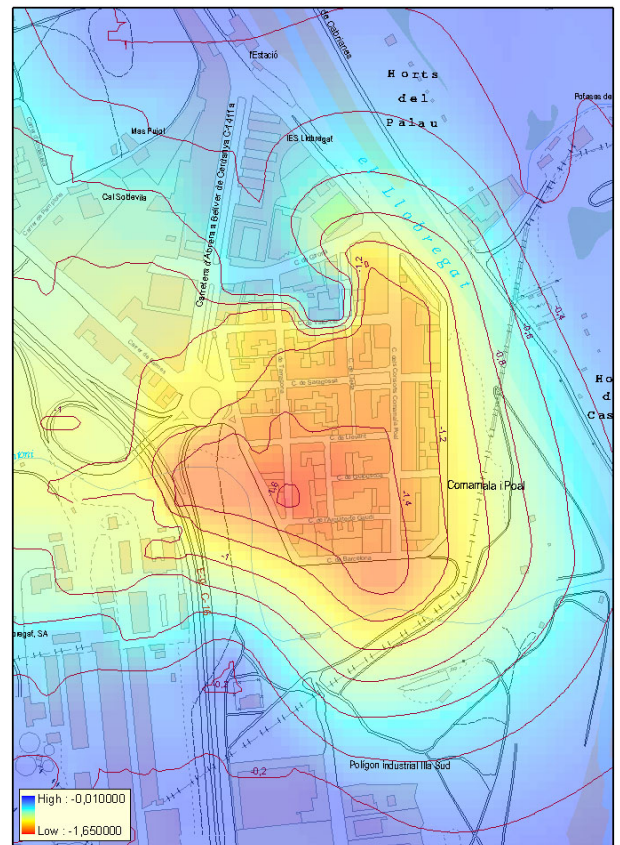


Figure 9. Velocity deformation values (cm/year) in a neighborhood of Sallent

Finally, Fig. 11 depicts all the areas in Catalonia where different levels of ground deformation have been detected.

Point	DInSAR	Leveling	Difference
5B	-1,14	-1,07	0,07
6	-1,18	-1,14	0,04
6A	-1,29	-1,27	0,01
6B	-1,19	-1,15	0,04
7	-1,37	-1,30	0,07
7B	-1,39	-1,32	0,06
16	-1,53	-1,55	-0,02
17	-1,75	-1,88	-0,12
A1	-1,21	-1,22	-0,01
A3	-1,54	-1,41	0,12

Table 3. Velocity comparison (cm/year) between advanced DInSAR and precise leveling measurements

## 6. CONCLUSIONS

This paper presents the DInSAR project that the ICC is carrying out for continuously monitoring terrain deformations in the Catalanian territory.

Some examples of deformation maps using classical and advanced DInSAR techniques are shown, demonstrating the suitability of radar satellites for monitoring large areas at a very low cost.

ICC's policy regarding this project is to acquire two additional images for each frame every year. Therefore, subsidence maps can be yearly updated for risk monitoring. Nevertheless, the available revisit period for ENVISAT satellite is not suitable for near real-time observations. This is a strong limitation for the applicability of these techniques for hazard monitoring. For this reason, a SAR satellite constellation with very short time intervals of acquisition is mandatory in a near future.

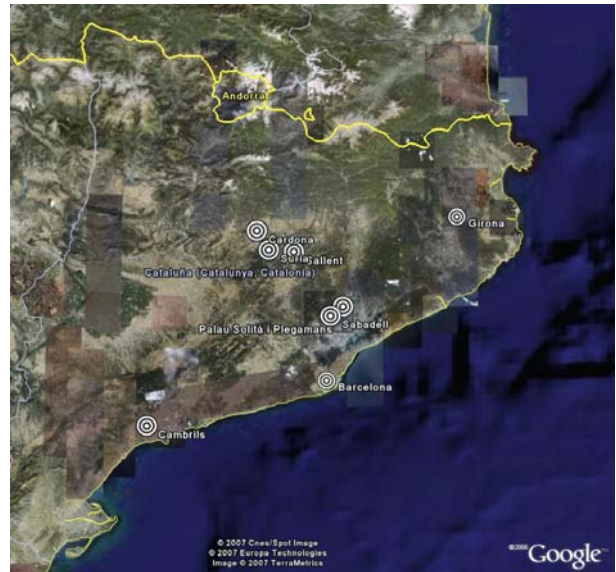


Figure 11. Catalanian zones affected by different levels of subsidence

## 7. REFERENCES

1. Pérez, F., Xandri, R., Arbiol, R., Palà, V. (2005). *Automatic Generation of Seamless Mosaics over Extensive Areas from High Resolution Imagery*, World Multi-Conference on Systemics, Cybernetics and Informatics (WMSCI), Orlando (USA).
2. Mora, O., Mallorquí, J.J., Broquetas, A. (2003). *Linear and Nonlinear Terrain Deformation Maps From a Reduced Set of Interferometric SAR Images*, IEEE Transactions on Geoscience and Remote Sensing, Vol. 41, No. 10.
3. Ferretti, A., Prati, C., Rocca, F. (2001). *Permanent scatterers in SAR interferometry*, IEEE Trans. on Geoscience and Remote Sensing, Vol. 39, No 1, pp. 8-30.
4. Berardino, P., Fornaro, G., Lanari, R., Sansosti E. (2002). *A New Algorithm for Surface Deformation Monitoring Based on Small Baseline Differential Interferograms*, IEEE Trans. on Geoscience and Remote Sensing, Vol. 40, No. 11, pp. 2375-2383.